Spin evolution in a two-dimensional electron gas after laser excitation

O. Morandi

Institute of Theoretical and Computational Physics, TU Graz, Petersgasse 16, A-8010 Graz, Austria

(Received 2 March 2011; revised manuscript received 16 May 2011; published 29 June 2011)

The femtosecond laser excitation of the spin configuration in a low-dimensional magnetic semiconductor is investigated. An atomistic Schrödinger model is developed in which trapped electrons and ionic impurities are coupled via exchange interactions. By defining a suitable set of non-Hermitian operators, the microscopic Schrödinger description of the particles is combined with the more phenomenological Landau-Bloch relaxation mechanism. Differing from the standard approaches, in this model the statistical widths of the wave functions become time-dependent. This enables the study of decoherence effects where the evolution of the system, from an initial pure state to a final mixed state, is induced by the spin interaction. Simulations reproduce the out-of-equilibrium spin evolution observed in ZnCdSe devices. The effects of quantum confinement and multimode excitation are discussed.

DOI: 10.1103/PhysRevB.83.224428 PACS number(s): 78.20.Ls, 78.30.Fs

I. INTRODUCTION

In the past few decades, an increasing effort has been devoted to designing new electronic nanodevices in which magnetic and electronic quantum structures coexist. The knowhow of band-gap engineering on semiconductor heterostructures has been widely exploited to devise some electrical control of the magnetic properties for these new materials.[1] Magnetism strongly influences the optical and transport properties of the confined electrons in these devices. The integration of magnetic and electronic quantum structures in a single device offers the interesting opportunity to obtain new physical insights into the spin transport and scattering in magnetic quantum semiconductors. Typically, microscopic control of the spin direction is achieved by confining particles or high-spin atoms into a small volume where an inhomogeneous magnetic field is present. This can be tailored by electrical control or by magnetic gates. The effect of magnetism on the confined electronic states emerges from temporally resolved magneto-optical spectroscopy, as well as magnetophotoluminescence, quantum magnetotransport, and the Kerr effect. Photodetection techniques that make use of a short laser pulse in thin-film samples are a well-established framework in which direct experimental access to the microscopic spin evolution in a micromagnet can be obtained.[2]

The spin coherence of electronic states is one of the key features involved in numerous concepts for spintronics devices (see, e.g., Ref. 3). Long spin lifetimes are a primary characteristic that a semiconductor should possess when the interest is focused on developing devices in which some efficient mechanisms for controlling the spin could be achieved. The spin coherence is often considerably longer compared with the coherence of the electronic wave function, which typically decays on the picosecond time scale. Many experimental studies are concentrated on n-type GaAs, where the spin-relaxation time is nearly 100 ns for the bulk and 10 ns for low-density GaAs quantum wells.[4,5] In any case, other materials such as CdTe- or InP-based quantum structures have lately received a great deal of attention.[6,7] They are being widely tested, and new information is available concerning the physical processes that limit the electron-spin coherence time.

The typical signal that can be extracted by magneto-optical spectroscopy is the evolution of the total magnetization of the sample after photoexcitation. In the case of wide channels (where the confining effect can be discarded), this signal can usually be fitted with a single damped sinusoidal oscillation. The spin precession is characterized only by the Larmor frequency and by the exponential decay. In some cases, the system shows a more various and interesting scenario in which quantum beat and multimode oscillations appear. These effects are typically induced by the presence of a spatially nonuniform magnetic field inside the device. In particular, the study of quantum beats (which were observed, for example, in some quantum-confined semiconductor nanostructures by Gerlovin's group in Ref. 7) is useful for detecting the fine structure of the energy states and for identifying the main mechanisms responsible for the decay of the spin coherence.[8]

However, the explanation of the latter mechanism is somehow controversial. For example, in the case of GaAs quantum wells doped with magnetic Mn acceptors, it is still not clear if the long spin memory should be attributed either to the spin dynamics of the ions or to the confined electron gas.[9,10] Other open questions also concern the influence of the Bir-Aronov-Pikus mechanism on the spin dynamics of bound electrons.[11]

When a confined system is considered, the exchange interaction between electrons and ions is modulated by the shape of the charge distribution. Consequently, each ion is exposed to a slightly different total magnetic field (and thus a Larmor precession). As a result, a nonconstant value of the mean precession frequency can be observed. The presence of a time-dependent Larmor frequency in some cases leads to a considerable increase of the Mn precession frequency.[12] Theoretical studies need to be done to clarify the origin of the observed dumping and multimode precession of the magnetization.

In particular, in Ref. 13, some experimental studies of spin dynamics were performed on a set of devices denoted "digital magnetic heterostructures." Based on the molecular-beam-epitaxy technique, they are composed of a series of equispaced MnSe layers grown in a ZnCdSe buffer, sandwiched between two ZnSe barriers. In these devices, the localized magnetic

spin of the Mn ions interacts strongly with the quantum-confined electronic states. The *sp-d* exchange interaction between the *d* electrons and the trapped electrons in ZnCdSe is antiferromagnetic, and in the presence of an external magnetic field, it enhances the spin splitting of the band states. Consequently, spin-up and spin-down states are pulled apart via the giant Zeeman effect,[14] and the system displays an overall magnetic order.

Experimental evidence suggests that the evolution of the total magnetization in a two-dimensional (2D) magnetic device and its macroscopic relaxation rate are strongly influenced by the spin-spin interaction between *sp* and *d* electrons.

Spatial inhomogeneity of the magnetic field, with particular attention given to the multimode oscillation regimes, has been analyzed recently in similar structures. In Ref. 12, it is shown that the presence of inhomogeneity of the magnetic fields in nano-ferromagnets constituted by a periodic array of (Zn,Cd,Mn)Se/ZnSe quantum wires of thickness 5 nm and with a channel length of the order of 0.5 μm leads to a magnetic response that differs qualitatively from the simple damped sinusoidal oscillation. In this system, as a result of the superposition of individual precessions with different frequencies about different axes, a temporal variation of the ensemble precession frequency is clearly observed, and the spin dephasing time is strongly reduced.[15] The coexistence of different collective spin-precession modes of the ionic spin is explained in terms of a semiclassical model. The mixed electron-ion spin modes are described within the mean-field approximation and represent the collective precession of the electron and ion spins either with the same or with opposite phases.[16]

Furthermore, the inhomogeneity of the magnetic field has also been considered by various groups as a new available degree of freedom that can be exploited to enhance some useful characteristics of the devices. For example, in this way, some coherent single-electron spin control can be achieved in a quantum dot[17] and a spin-selective trap for carriers in diluted magnetic semiconductors was proposed.[18]

Different approaches, including Green's functions[19,20] and some semiphenomenological formulations,[2] have been proposed to simulate the spin evolution in a magnetic device by applying an external source of perturbation. Most of the theoretical investigations of the magnetization dynamics are based on a micromagnetic approach that considers the magnetization of a particle in terms of a classical-type vector of a fixed length subjected to the phenomenological Landau equation. Within this context, quantum confinement cannot be reproduced, and the effect of an electric field is included at the classical level.

In this paper, we propose a model for the coupled evolution of magnetic ions and trapped particles in which the effects of the confining potential are reproduced in a full quantum context. We apply our model to study the spin evolution in ZnCdSe devices driven out-of-equilibrium by laser excitation.

II. MODEL

We consider an electron gas trapped in a Mn-doped heterostructure in the presence of an external magnetic field **B**. When the spatial confinement of the charge carriers is discarded, the atomistic models provide a valuable approach to reproduce the particle spin evolution in the presence of a magnetic field, external or mediated by exchange interaction. In this context, the statistical mixture of spin particles is described by a vector **S**, whose length is proportional to the spin polarization of the particle gas. Based on very general assumptions, with Ref. 21, we consider the following equation for the spin density $\mathbf{s} = n^h \mathbf{S}$ (where n^h denotes the density of particles):

$$\frac{d\mathbf{s}}{dt} = -\mathbf{s} \wedge \left(\mathbf{B}^S - n^h \alpha(\mathbf{s}) \frac{\mathbf{s} \wedge \mathbf{B}^S}{|\mathbf{s}|^2} \right) - \Lambda \left(1 - \frac{\mathbf{s} \cdot \mathbf{B}^S}{|\mathbf{B}^S||\mathbf{s}_{\rm eq}|} \right) \mathbf{s}, \tag{1}$$

where

$$\mathbf{B}^S = \left(\frac{J_{pd}}{2} \mathbf{m} + \frac{g \mu_B}{\hbar} \mathbf{B} \right) . \tag{2}$$

Here, J_{pd} denotes the exchange constant, α and Λ are the Landau damping parameters, g stands for the Landé g factor, and μ_B denotes the Bohr magneton. $\mathbf{s}_{\rm eq}$ is the equilibrium spin distribution whose explicit form is derived in Eq. (B3). We used $\mathbf{m} = \mathbf{m}(\mathbf{r},t)$ to indicate the local Mn-moment magnetization. Equation (1) includes energy dissipation and the alignment of the electron spin toward $\mathbf{B}^S$ (see Ref. 21 for a discussion of this term). We refer to this equation of motion as the Landau-Lifshitz-Bloch (LBB) equation.

In the problem with which we are concerned, the system is represented by a two-dimensional (2D) electron gas trapped in a quantum-well heterostructure with Mn doping. Under these assumptions, the quantum effects induced by the confining potential cannot be discarded, and a more fundamental approach than Eq. (1) has to be considered. From a microscopic point of view, the quantum-mechanical mixed state is defined by a set of wave functions ψ_i with statistical width p_i, and the evolution of the spin density is described by the Schrödinger equation. The mean spin density **s** of the system is

$$\mathbf{s} = \sum_i p_i \mathbf{S}_i, \tag{3}$$

$$\mathbf{S}_i = \tfrac{1}{2} \langle \psi_i | \boldsymbol{\sigma} | \psi_i \rangle, \tag{4}$$

where $\boldsymbol{\sigma}$ is the Pauli vector matrix.

We state the following result: given a set of wave functions $\psi_i(\mathbf{r},t)$ and statistical width $p_i(t)$, which are solutions of the system (see Appendix A for the definition of $p_{\bar{i}}$)

$$\frac{\partial \psi_i}{\partial t} = \frac{1}{\hbar} (-i\, \mathbf{H} \cdot \boldsymbol{\sigma} + \mathbf{G}_i \cdot \boldsymbol{\sigma} + \widetilde{G}_i\, \sigma_0) \psi_i, \tag{5}$$

$$\frac{\partial p_i}{\partial t} = (p_i - p_{\bar{i}}) \frac{1}{2} \int \mathfrak{G}(\mathbf{s},\mathbf{r}) |\psi_i|^2 \, d\mathbf{r} , \tag{6}$$

where σ_0 is the 2×2 identity matrix and

$$\mathbf{G}_i(\mathbf{r}) = \frac{\hbar}{|\psi_i|^2} \mathfrak{G}(\mathbf{s},\mathbf{r}) \mathbf{S}_i , \tag{7}$$

$$\widetilde{G}_i = -\frac{\hbar}{2\|\psi_i\|^2} \int \mathfrak{G}(\mathbf{s},\mathbf{r}) |\psi_i|^2 \, d\mathbf{r} , \tag{8}$$

the mean spin density, defined in Eq. (3), satisfies the following macroscopic equation:

$$\frac{d\mathbf{s}}{dt} = \frac{1}{\hbar}\mathbf{s} \wedge \mathbf{H} + \mathfrak{G}(\mathbf{s},\mathbf{r})\mathbf{s} \tag{9}$$

with initial conditions

$$\mathbf{s}(t_0) = \frac{1}{2}\sum_i p_i(t_0)\langle\psi_i(t_0)|\boldsymbol{\sigma}|\psi_i(t_0)\rangle \ . \tag{10}$$

Here, the vector field $\mathbf{H}$ and the functional $\mathfrak{G}$ are given. Moreover, the usual conservation of ψ norm and the total mass of the system hold true,

$$\frac{d}{dt}\|\psi_i(t)\| = 0, \tag{11}$$

$$\frac{dN}{dt} = \sum_i^N \frac{dp_i}{dt} = 0. \tag{12}$$

Details of the derivation of Eqs. (5) and (6) are given in Appendix A.

We consider the system of Eqs. (5) and (6) as a convenient tool for modeling the spin evolution of a magnetic device, where the microscopic Schrödinger framework can be combined with the more phenomenological atomistic approach. In particular, we exploit Eqs. (5) and (6) to include the Landau-Bloch spin relaxation mechanism, in the usual equation of motion for the electron spin.

The main idea of the previous result was to define two non-Hermitian operators $\mathbf{G}_i(\mathbf{r})$, $\widetilde{G}_i$ such that Eq. (1) is satisfied and, at the same time, the conservation of the ψ norm and the total mass of the system is ensured. Usually, when the Schrödinger formalism is applied to open systems, the statistical width are *a priori* fixed and are chosen independently of the wave evolution equation (for example, they are obtained by estimating the influx or diffusion of particles entering in the device through the boundaries, or are related to the mean value of some observable). In our approach, we compensate the overall loss of mass induced by the presence of the non-Hermitian operators $\mathbf{G}_i(\mathbf{r})$, $\widetilde{G}_i$, by letting the statistical widths p_i have some time dependence. One of the improvements provided by the present extension to the standard ballistic Schrödinger approach is the possibility of studying decoherence effects in which some interactions (spin interaction in our case) lead the system to evolve from an initial pure state to a final mixed state.

Finally, a straightforward extension of the Schrödinger-like Eq. (5) allows us to include in a unique equation both the effects of the lattice Hamiltonian $\mathcal{H}_h$ and the LBB Eq. (1). We have

$$i\hbar\frac{\partial\psi_i}{\partial t} = \left[\mathcal{H}_h - \left(\mathbf{B}^S - n^h\alpha\frac{\mathbf{s}\wedge\mathbf{B}^S}{|\mathbf{s}|^2} + i\mathbf{G}_i\right)\cdot\boldsymbol{\sigma} + i\widetilde{G}_i\sigma_0\right]\psi_i, \tag{13}$$

$$\mathbf{B}^S = \left(\frac{J_{pd}}{2}\mathbf{m} + \frac{g\mu_B}{\hbar}\mathbf{B}\right) ,$$

where $\mathbf{G}_i(\mathbf{r})$, $\widetilde{G}_i$ are given by Eqs. (7) and (8) with

$$\mathfrak{G} = -\Lambda\left(1 - \frac{\mathbf{s}\cdot\mathbf{B}^S}{|\mathbf{s}_{\rm eq}|\ |\mathbf{B}^S|}\right) \ . \tag{14}$$

The time evolution Eq. (6) is unchanged,

$$\frac{\partial p_i}{\partial t} = (p_i - p_{\bar{i}})\frac{1}{2}\int \mathfrak{G}|\psi_i|^2\, d\mathbf{r} \ . \tag{15}$$

We include in our model also the evolution of the ion magnetization $\mathbf{m}$ by means of the following Landau equation:

$$\frac{d\mathbf{m}}{dt} = -\mathbf{m}\wedge\mathbf{B}^M \tag{16}$$

with

$$\mathbf{B}^M = \frac{J_{pd}}{2}\mathbf{s} + \frac{g\mu_B}{\hbar}\mathbf{B}. \tag{17}$$

We remark that, motivated by the experimental finding of Ref. 13, in this contribution we do not include any ion spin relaxation mechanism that acts directly on $\mathbf{m}$. In these optical experiments, spin relaxation and coherent spin transport in undoped magnetic semiconductors are probed, revealing relaxation times for the ion spin of the order of nanoseconds (that can be considered negligible in the time scale in which the total magnetization evolves).

III. NUMERICAL RESULTS

Equations (13)–(16) have been solved numerically (we apply a second-order Crank-Nicolson scheme) with the aim of studying the role of the quantum confinement on the dynamics of the magnetization after laser irradiation. We consider a sample composed of a 12 nm $Zn_{0.77}Cd_{0.23}Se/ZnSe$ single quantum well, containing uniform concentrations of Mn^{2+} ions. An external magnetic field $\mathbf{B}$ is applied along the confining direction (z axis). At equilibrium, the sample displays a net magnetization directed along $\mathbf{B}$. This results from the strong antiferromagnetic coupling between ions and sp electrons that overcomes the d-d superexchange interaction between the d electrons of the magnetic ions (at low temperature, the presence of an external field is not strictly necessary to generate an ordered ferromagnetic configuration, but mainly to avoid the formation of magnetic walls). Hence, the magnetism is mediated by the presence of the particles (typically a small concentration) trapped in the quantum well, and enhances the spin splitting of the band states when an external magnetic field is applied (giant Zeeman effect). In Fig. 1 (left panel), we report the stationary distribution of electrons before the laser heating, evaluated by using the mean-field Zener model,[14] for a particle density $n^h = 10^{11}$ cm^{-2}, 5% Mn-ion concentration, at a temperature $T = 4.5$ K and for $|\mathbf{B}| = 0.1$ T. In the right panel of Fig. 1, the self-consistent hole band edge profile is represented (the Coulomb repulsion between the electrons is taken into account by using the standard mean-field Hartree approximation). The horizontal line denotes the position of the chemical potential and the crosses represent the energies of the resonant levels.

The spin dynamics is triggered by ultrashort laser excitation. Concerning the setup of the irradiation, we consider a Voigt geometry, for which the direction of the light propagation (x axis) is orthogonal to the magnetic field (z axis). At $t = 0$, a femtosecond circularly polarized optical pulse impacts the device creating a hot quasithermal distribution $n^{\rm ex}$ of spin-polarized particles in the quantum well. In particular, by varying the light polarization, many different spin excitations

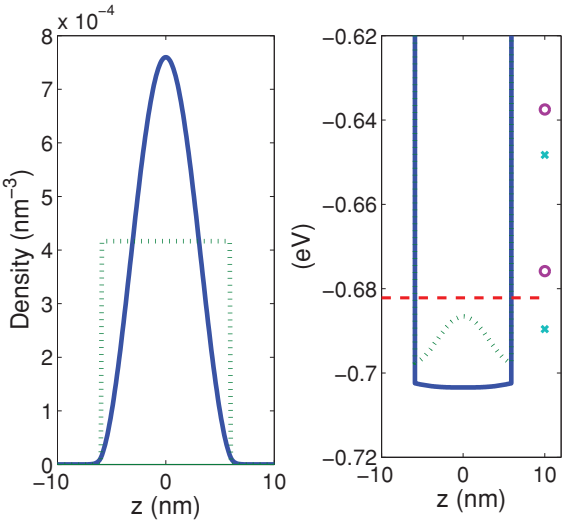

FIG. 1. (Color online) (Left panel) Stationary distribution of the charge (continuous blue line) and doping profile (dashed green line) in the 12 nm $Zn_{0.77}Cd_{0.23}Se/ZnSe$ quantum well. (Right panel) spin-up (continuous blue line) and spin-down self-consistent potential (dashed green line). Crosses and circles mark the resonant states inside the well. The temperature is 4.5 K.

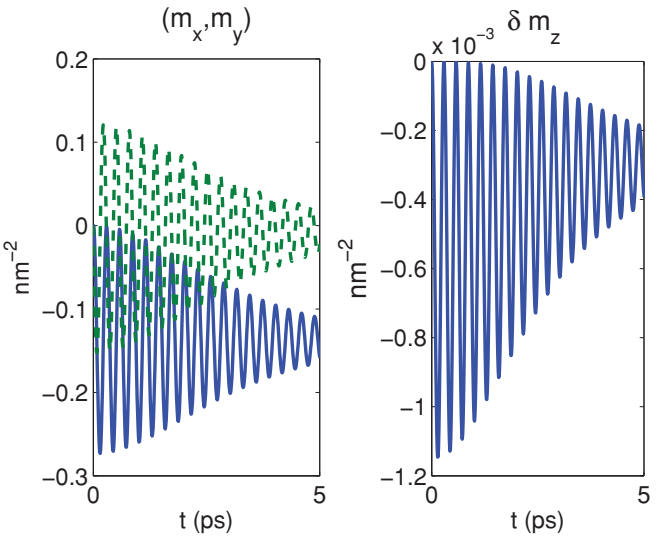

FIG. 3. (Color online) Left plot: continuous blue line (dashed green line): time evolution of the x (y) component of the total spin polarization of ions $\overline{\mathbf{m}}$. Right plot: $\delta m_z \equiv \overline{m}_z(t) - \overline{m}_z(t_0)$. The initial magnetization $\overline{m}_z(t_0)$ is equal to 49.89 nm^{-2}.

are possible. In our simulation, we assume that the initial spin polarization of the photocreated particle is directed along the x axis. Since the electron spin is quantized along the magnetic field, photoinjecting electrons with definite spin direction corresponds to pumping a coherent superposition of the spin-split electron states. Consistent with the experimental finding presented by the Awschalom group,[22] Figs. 2 and 3 show that the out-of-plane components of the ions spin, precess with a period of the order of 300 fs, and decay within 2 ps. We stress that despite the fact that no relaxation mechanism is directly inserted in the evolution of the ion spin [see Eq. (16)], our model predicts the correct damping ratio of the ion magnetization. Natural decay of the ion spin in the absence of trapped electrons is found in the much higher time scale of nanoseconds. The relaxation of ions spin is induced only by trapped electrons via exchange mechanisms. Since (as already analyzed in previous contributions[20,23]) the spin-flip exchange mechanism between ions and electrons is particularly efficient, the Landau relaxation process, mediated by the 2D electron gas, becomes the dominant relaxation mechanism of the ion spin. In our simulations, we used $\alpha = 10^{-3}$ J_{pd} and $\Lambda = 0$. In Fig. 4, we present the long-time behavior of the ion magnetization. The simulation shows that after the electron spin has become completely aligned with the total mean magnetization via the Landau decay, a smoother residual oscillation (whose period is of the order of 50 ps) is still present. In this final part of the numerical experiment, the system is in a

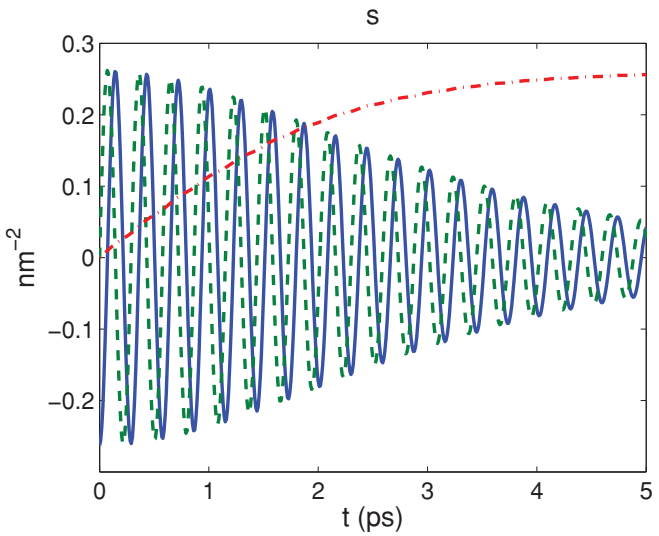

FIG. 2. (Color online) Time evolution of the total spin polarization of the trapped particles $\overline{\mathbf{s}}$. Continuous blue line, $\overline{s}_x$; dashed green line, $\overline{s}_y$; dot-dashed red line, $\overline{s}_z$.

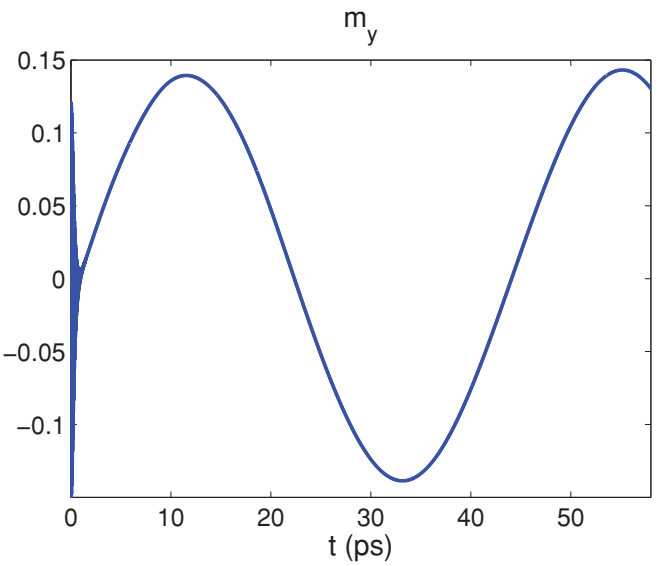

FIG. 4. (Color online) Long-time behavior of $\overline{\mathbf{m}}_y$.

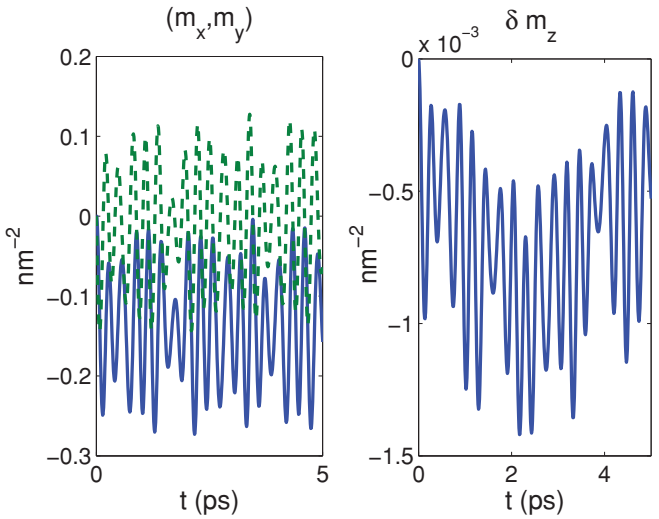

FIG. 5. (Color online) Left plot, continuous blue line (dashed green line): time evolution of the x (y) component of the total spin polarization of ions $\overline{\mathbf{m}}$. Right plot: $\delta m_z \equiv \overline{m}_z(t) - \overline{m}_z(t_0)$. The initial magnetization $\overline{m}_z(t_0)$ is equal to 49.89 nm^{-2}. Here the simulation is performed in the absence of Landau damping.

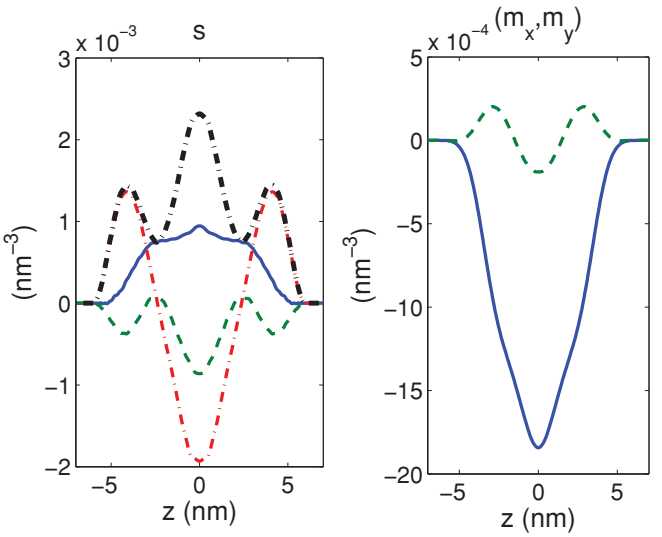

FIG. 6. (Color online) Left panel: x (continuous blue line), y (dashed green line), and z (dot-dashed red line) components of $\bar{\mathbf{s}}$ for $t = 0.3$ ps. The dot-dashed black line represents the modulus of $\bar{\mathbf{s}}$. Right panel: x (continuous blue line) and y (dashed green line) components of $\overline{\mathbf{m}}$ for $t = 0.3$ ps.

quasiequilibrium state and the out-of-plane laser-excited magnetization, which is not completely damped, oscillates around $\mathbf{B}$. These results are confirmed by the experiment performed in Ref. 22.

The form of the charge profile of the 2D trapped gas along the confining direction has interesting effects on the overall spin evolution of the system. In contrast to the various mean-field methods, in our approach we combine the full quantum microscopic description of the confining heterostructure profile with the Landau-like spin-relaxation effect. Nonuniform distributions of the magnetic field along the z axis can thus be easily investigated. Despite the presence of a uniform distribution of ions along the channel, the statical polarization of their spin is not uniform and reflects the sinusoidal shape of the trapped eigenstates. At equilibrium, the ion spin polarization is given by $\mathbf{m}_{\rm eq}(\mathbf{r}) = \frac{\mathbf{B}^M}{|\mathbf{B}^M|} m_{\rm eq}$, where

$$m_{\rm eq} = \frac{5}{2}\mathcal{B}_{5/2}\left[\frac{5}{2k_BT}|\mathbf{B}^M|\right], \tag{18}$$

$\mathcal{B}_{5/2}$ is the Brillouin function, k_B is the Boltzmann constant, T is the temperature, and $\mathbf{B}^M$ is defined in Eq. (17).[24] In this formula, the dominant term is the exchange contribution, which is proportional to the charge density inside the well. As a consequence, the giant Zeeman splitting is not uniform, and particles in the center of the device suffer from a major exchange field with respect to those that are close to the junction, where the wave function vanishes exponentially. When the out-of-equilibrium spin distribution is excited, the torque force acting on both spin populations (ions and trapped electrons) is stronger where trapped particles cumulate and increases the Larmor precession there. The overall mean spin polarization is a mixture of spin precessing with different angular frequencies, and will be consequently reduced by interference effects between slow- and fast-rotating components of the spin.

To provide evidence for this aspect, in Fig. 5 we show the evolution of the total magnetization in the absence of any Landau spin-relaxation process (and we artificially increase the effective electron mass from 0.16 to 1). The interference effects give rise to a complex evolution path of the total magnetization, where $\mathbf{m}$ beats in a period of 1 ps. To illustrate the strong inhomogeneity of the magnetization along the z axis, in Fig. 6 we display the distribution of the electron and ion magnetization after one oscillation period of $\mathbf{m}$ (corresponding to $t = 0.3$ ps).

In Fig. 7, we depict the evolution of the trapped electron magnetization for different laser excitations. In the previous simulations, we assumed a monoenergetic laser beam tuned to the first resonant state. By letting the density of photocreated

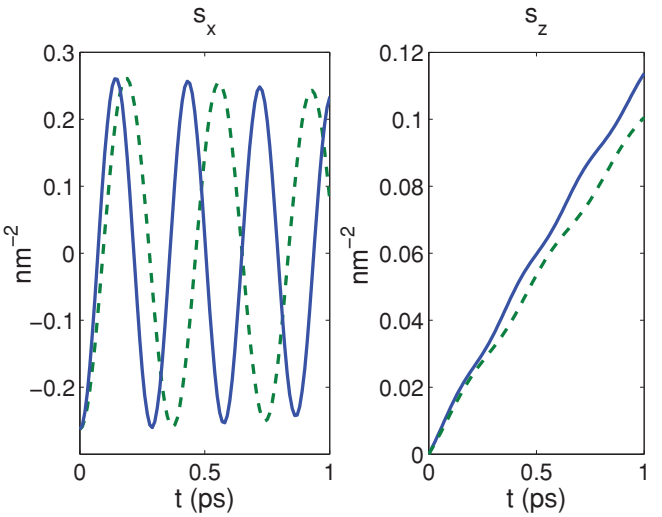

FIG. 7. (Color online) Time evolution of $\bar{\mathbf{s}}$: left panel, $\bar{s}_x$; right panel, $\bar{s}_z$. Continuous blue line and dashed green line refer to the first and second resonant state excitation, respectively.

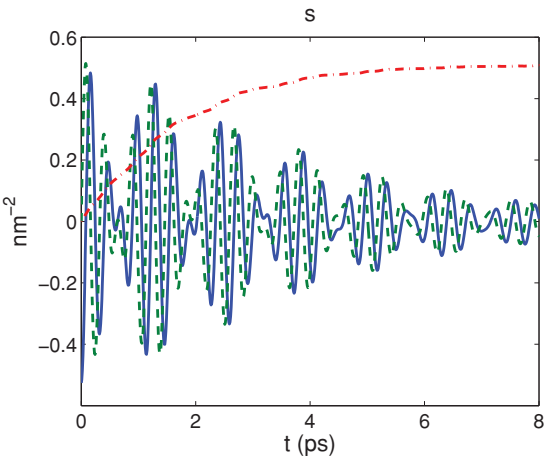

FIG. 8. (Color online) Time evolution of $\bar{\mathbf{s}}$. Continuous blue line: $\bar{s}_x$, dashed green line: $\bar{s}_y$, dot-dashed red line: $\bar{s}_z$.

particles $n^{\mathrm{ex}} = 10^{10}$ cm^{-2}, we increase the laser frequency to excite higher resonant states. Figure 7 shows the difference of the oscillation frequencies between the first and second resonant state. Since a frequency spread is always present in a real laser excitation, a realistic modeling of the laser pulse should consider the simultaneous excitation of more than a single resonant state. In Figs. 8 and 9, we display the evolution of the magnetization in the hypothesis that the first two resonant states are excited equally. The simulation shows that the envelope of the magnetization is modulated by a second-harmonic frequency with a period of the order of 1.5 ps. We remark that, with respect to the evolution of the total magnetization, the excitation of two different resonant states is a nonlinear process, which generates multiple harmonic mixing.

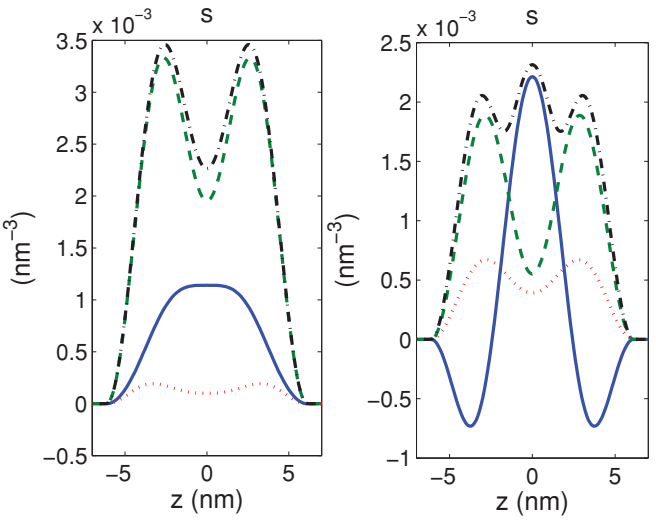

FIG. 9. (Color online) Here, x (continuous blue line), y (dashed green line), and z (dot-dashed red line) are the components of $\bar{\mathbf{s}}$ for $t = 0.3$ ps. The dot-dashed black line represents the modulus of $\bar{\mathbf{s}}$. Left panel: $t = 0.08$ ps, right panel: $t = 0.4$ ps.

IV. CONCLUSION

The effect of laser excitation on the spin configuration in a magnetic semiconductor is investigated by applying an atomistic Schrödinger approach. Our model reproduces the initial coherent rotation of the Mn^{2+} moments (initially oriented along the applied **B** field) induced by the torque effect of the strong exchange field generated by the excited spin. Simulations show a terahertz spin precession of photoinjected electrons, accompanied by a relaxation, and provide a simple explanation of the physical processes underlying the picosecond precession and damping of the total magnetization of the sample. The principal results of the present contribution concern the study of ion-spin relaxation mediated by spin-exchange mechanisms, the effect of the quantum confinement, and multimode excitation.

ACKNOWLEDGMENTS

This work has been supported by the Austrian Science Fund, Vienna, under Contract No. P 21326 - N 16.

APPENDIX A: COMPATIBILITY BETWEEN THE LBB EQUATION AND THE MACROSCOPIC SPIN DUMPING FORMULA

We show the equivalence between the macroscopic formulation of the mean spin density evolution given by Eq. (9) and the Schrödinger evolution Eq. (5), by deriving Eqs. (6)–(8). Given a set of wave functions ψ_i and statistical width p_i, from the definition of $\mathbf{S}_i$ in Eq. (4) and from Eq. (5) it is easy to verify that Eq. (9) is satisfied if

$$\sum_i \left(\frac{\partial p_i}{\partial t} + p_i \frac{2\widetilde{G}_i}{\hbar} \right) \mathbf{S}_i + \sum_i \left(\frac{1}{\hbar} \mathbf{G}_i |\psi_i|^2 - \mathfrak{G}(\mathbf{s}) \mathbf{S}_i \right) p_i = 0. \tag{A1}$$

The second bracket vanishes if, according to Eq. (8), we fix $\mathbf{G}_i(\mathbf{r})$ as

$$\mathbf{G}_i(\mathbf{r}) = \frac{\hbar}{|\psi_i|^2} \mathfrak{G}(\mathbf{s}) \mathbf{S}_i .$$

By imposing the conservation of the norm given by Eq. (11), we obtain Eq. (7),

$$\widetilde{G}_i = -\frac{2}{\|\psi_i\|^2} \int \mathbf{G}_i \cdot \mathbf{S}_i \, d\mathbf{r} = -\frac{\hbar}{\|\psi_i\|^2} \frac{1}{2} \int \mathfrak{G}(\mathbf{s}) |\psi_i|^2 \, d\mathbf{r}, \tag{A2}$$

where we used

$$|\mathbf{S}_i| = \tfrac{1}{2} |\psi_i|^2. \tag{A3}$$

Equation (A1) becomes

$$\sum_i \left(\frac{\partial p_i}{\partial t} - \frac{p_i}{\|\psi_i\|^2} \int \mathfrak{G}(\mathbf{s}) |\psi_i|^2 \, d\mathbf{r} - k_i \right) \mathbf{S}_i = 0, \tag{A4}$$

where we choose a set of k_i coefficients such as

$$\sum_i^N k_i \mathbf{S}_i = 0. \tag{A5}$$

The previous equation is automatically fulfilled if we assume that to each kth state corresponds a $\bar{k}$ state such as

$$\mathbf{S}_i = -\mathbf{S}_{\bar{i}}. \tag{A6}$$

Equation (A5) gives

$$\sum_i^{N/2} (k_i - k_{\bar{i}})\mathbf{S}_i = 0 \tag{A7}$$

or $k_i = k_{\bar{i}}$. All we have to do to is, at $t = 0$, to associate to each wave function $\psi_i(t_0)$ a state $\psi_{\bar{i}}$ such that Eq. (A6) is satisfied. It is easy to verify that for all the couples of functions $(\psi_i, \psi_{\bar{i}})$, Eq. (A6) remains satisfied for all t. From Eq. (A4), we have

$$\frac{\partial p_i}{\partial t} = \frac{p_i}{\|\psi_i\|^2} \int \mathfrak{G}(\mathbf{s})|\psi_i|^2 \, d\mathbf{r} + k_i. \tag{A8}$$

The time derivative of the total number of particles is

$$\frac{\partial N}{\partial t} = \sum_i^N \frac{\partial p_i}{\partial t} = \sum_i^{N/2} \frac{1}{\|\psi_i\|^2} \times \left(p_i \int \mathfrak{G}(\mathbf{s})|\psi_i|^2 \, d\mathbf{r} + p_{\bar{i}} \int \mathfrak{G}(\mathbf{s})|\psi_{\bar{i}}|^2 \, d\mathbf{r} \right) + 2k_i \tag{A9}$$

and we have conservation $\frac{\partial N}{\partial t} = 0$ if

$$k_i = -\frac{1}{2\|\psi_i\|^2} \left(p_i \int \mathfrak{G}(\mathbf{s})|\psi_i|^2 \, d\mathbf{r} + p_{\bar{i}} \int \mathfrak{G}(\mathbf{s})|\psi_{\bar{i}}|^2 \, d\mathbf{r} \right), \tag{A10}$$

$$\frac{\partial p_i}{\partial t} = \frac{1}{2\|\psi_i\|^2} p_i \int \mathfrak{G}(\mathbf{s})|\psi_i|^2 \, d\mathbf{r} - \frac{1}{2\|\psi_i\|^2} p_{\bar{i}} \times \int \mathfrak{G}(\mathbf{s})|\psi_{\bar{i}}|^2 \, d\mathbf{r}, \tag{A11}$$

and thus we obtain Eq. (6). Moreover, Eqs. (A6) and (A3) give

$$|\psi_{\bar{i}}|^2 = |\psi_i|^2 \, . \tag{A12}$$

APPENDIX B: EQUILIBRIUM HOLE SPIN DISTRIBUTION

We derive the formula that describes the equilibrium spin distribution of the holes used in Eq. (1). The Zener model provides a quite well established approach that reproduces the ion-electron equilibrium state in a confined semiconductor heterostructure with diluted magnetic doping. This model has been applied to different host materials (see, e.g., Refs. 14,25–27), and in the case of digital magnetic Zn/Se(Zn,Cd)Se heterostructures, its theoretical prediction of the value of the hole spin-splitting energy has been experimentally confirmed.[28] The model consists of a nonlinear Schrödinger problem, where the 2D electron gas is spin-polarized by an external magnetic field. The polarization effect is strongly enhanced by the presence of the $sp - d$ exchange interaction between the holes and the magnetic ions. The latter is evaluated under the hypothesis that the magnetic ions are also polarized by the electron gas and behave like independent paramagnetic 5/2 spin particles. For the sake of simplicity, we consider here only the hh band in the effective-mass approximation (see Ref. 22 for the justification of this assumption). In this case, the Zener model consists of the stationary Schrödinger equation associated with Eq. (13) (without any dynamical dumping factor),

$$\left[\mathcal{H}_h - \left(\frac{J_{pd}}{2} \mathbf{m} + \frac{g\mu_B}{\hbar} \mathbf{B} \right) \cdot \boldsymbol{\sigma} \right] \phi_{\mathbf{k},i} = \varepsilon_{\mathbf{k},i} \phi_{\mathbf{k},i} \, , \tag{B1}$$

where $\mathbf{k}$ indicates the components of the momentum parallel to the sample and i is the subband index. We denote the spin component of the eigenstates with $\phi_{\mathbf{k},i} = \phi^{\uparrow}_{\mathbf{k},i}|\uparrow\rangle + \phi^{\downarrow}_{\mathbf{k},i}|\downarrow\rangle$, where the spin states are projected along the direction of the external magnetic field. Under the effective-mass approximation, each eigenstate is also a spin eigenstate. We can thus classify the solutions in terms of the indices $i = (b,\sigma)$, where b denotes the miniband and σ the spin. The equilibrium spin density is given by

$$s_{eq} = \sum_i \frac{1}{2} \int e^{-\frac{1}{k_B T}(\mu + \varepsilon^0_{\mathbf{k},b})} \left[e^{-\frac{\Delta\varepsilon_b}{k_B T}} |\phi^{\uparrow}_{\mathbf{k},b}|^2 - e^{\frac{\Delta\varepsilon_b}{k_B T}} |\phi^{\downarrow}_{\mathbf{k},b}|^2 \right] d\mathbf{k}, \tag{B2}$$

where μ is the chemical potential. Further, we defined $2\varepsilon^0_{\mathbf{k},b} = \varepsilon_{\mathbf{k},b,\uparrow} + \varepsilon_{\mathbf{k},b,\downarrow}$, $2\Delta\varepsilon_b = \varepsilon_{\mathbf{k},b,\uparrow} - \varepsilon_{\mathbf{k},b,\downarrow}$ (under the effective-mass approximation, it is easy to see that $\Delta\varepsilon_b$ does not depend on $\mathbf{k}$), and dropped for simplicity the lower spin index in the wave function: $\phi^{\sigma}_{\mathbf{k},b} \equiv \phi^{\sigma}_{\mathbf{k},b,\sigma}$ with $\sigma = \uparrow \, , \downarrow$.

Although it is possible in principle to use in our dynamical model formula (B2) to estimate the equilibrium spin density, the numerical cost required for the eigenvalue problem of Eq. (B1) is quite high and the direct use of the Zener model for the calculation of s_{eq} is no longer convenient for our purposes. A look at Eq. (B2) reveals that if we assume that for each band the shape of the eigenvectors of spin up and spin down is similar ($|\phi^{\uparrow}_{\mathbf{k},b}|^2 \simeq |\phi^{\downarrow}_{\mathbf{k},b}|^2$), the equilibrium spin density simplifies considerably, giving

$$s_{\mathrm{eq}} \simeq \sum_b \frac{n^h_b}{2} \mathcal{B}_{1/2}(\Delta\varepsilon_b), \tag{B3}$$

where

$$n^h_b = \left[e^{-\frac{\Delta\varepsilon_b}{k_B T}} + e^{\frac{\Delta\varepsilon_b}{k_B T}} \right] \int e^{-\frac{1}{k_B T}(\mu + \varepsilon^0_{\mathbf{k},b})} |\phi_{\mathbf{k},b}|^2 \, d\mathbf{k} \tag{B4}$$

is the particle density in the bth miniband. In formula (B3), the only relevant parameter is the spin-splitting energy $\Delta\varepsilon_b$. An empirical formula that estimates $\Delta\varepsilon_b$ and agrees with experimental results for a quite large interval of the external magnetic-field strength and doping concentration is provided by[22,28]

$$\Delta\varepsilon_b \simeq g\mu_B|\mathbf{B}| + c \, n^{\mathrm{Mn}} J_{pd} \, m_{\mathrm{eq}}(T_{\mathrm{eff}}), \tag{B5}$$

where m_{eq} is given by Eq. (18). Here, g is the effective g factor, n^{Mn} is the ion concentration, c stands for the overlap between the wave function of the hole states and the d orbitals, and $T_{\mathrm{eff}} = T + T_0$ is a modified temperature. In Eq. (B5), T_0 and c are treated as fitting parameters and the spin splitting is constant for all the minibands. By assuming the phenomenological law (B5), the local equilibrium hole

spin density becomes

$$s_{\rm eq} = \frac{n^h}{2}\mathcal{B}_{1/2}(\Delta\varepsilon). \tag{B6}$$

We remark that, despite its simplicity, this formula is not completely trivial since $s_{\rm eq}$ depends on the instantaneous hole spin polarization $\mathbf{s}(t)$ via $m_{\rm eq}$.

[1] G. A. Prinz, Science **250**, 1092 (1990).
[2] E. Beaurepaire, J.-C. Merle, A. Daunois, and J.-Y. Bigot, Phys. Rev. Lett. **76**, 4250 (1996).
[3] *Semiconductor Spintronics and Quantum Computation*, edited by D. D. Awschalom, D. Loss, and N. Samarth (Springer-Verlag, Berlin, 2002).
[4] J. M. Kikkawa and D. D. Awschalom, Phys. Rev. Lett. **80**, 4313 (1998).
[5] R. I. Dzhioev, V. L. Korenev, B. P. Zakharchenya, D. Gammon, A. S. Bracker, J. G. Tischler, and D. S. Katzer, Phys. Rev. B **66**, 153409 (2002).
[6] E. A. Zhukov, D. R. Yakovlev, M. Bayer, G. Karczewski, T. Wojtowicz, and J. Kossut, Phys. Status Solidi B **243**, 878 (2006).
[7] I. Ya. Gerlovin, I. V. Ignatiev, I. A. Yugova, and Y. Masumoto, Opt. Spectrosc. **104**, 577 (2008).
[8] S. Bar-Ad and I. Bar-Joseph, Phys. Rev. Lett. **66**, 2491 (1991).
[9] G. V. Astakhov, R. I. Dzhioev, K. V. Kavokin, V. L. Korenev, M. V. Lazarev, M. N. Tkachuk, Yu. G. Kusrayev, T. Kiessling, W. Ossau, and L. W. Molenkamp, Phys. Rev. Lett. **101**, 076602 (2008).
[10] R. C. Myers, M. H. Mikkelsen, J. M. Tang, A. C. Gossard, M. E. Flatte, and D. D. Awschalom, Nat. Mater. **7**, 203 (2008).
[11] I. A. Akimov, R. I. Dzhioev, V. L. Korenev, Yu. G. Kusrayev, E. A. Zhukov, D. R. Yakovlev, and M. Bayer, Phys. Rev. B **80**, 081203(R) (2009).
[12] P. E. Hohage, J. Nannen, S. Halm, J. Puls, F. Henneberger, and G. Bacher, J. Supercond. Nov. Magn. **23**, 135 (2010).
[13] D. D. Awschalom and N. Samarth, Solid State Commun. **107**, 663 (1998).
[14] T. Dietl, H. Ohno, F. Matsukura, J. Cibert, and D. Ferrand, Science **287**, 1019 (2000).
[15] S. Halm, P. E. Hohage, J. Nannen, G. Bacher, J. Puls, and F. Henneberger, Phys. Rev. B **77**, 121303(R) (2008).
[16] M. Vladimirova, S. Cronenberger, P. Barate, D. Scalbert, F. J. Teran, and A. P. Dmitriev, Phys. Rev. B **78**, 081305(R) (2008).
[17] Y. Tokura, W. G. van der Wiel, T. Obata, and S. Tarucha, Phys. Rev. Lett. **96**, 047202 (2006).
[18] P. Redlinski, T. Wojtowicz, T. G. Rappoport, A. Libal, J. K. Furdyna, and B. Janko, Phys. Rev. B **72**, 085209 (2005).
[19] M. D. Kapetanakis and I. E. Perakis, Phys. Rev. Lett. **101**, 097201 (2008).
[20] O. Morandi and P.-A. Hervieux, Phys. Rev. B **81**, 195215 (2010).
[21] D. A. Garanin, Phys. Rev. B **55**, 3050 (1997).
[22] D. D. Awschalom and N. Samarth, J. Magn. Magn. Mater. **200**, 130 (1999).
[23] O. Morandi, P.-A. Hervieux, and G. Manfredi, New J. Phys. **11**, 073010 (2009).
[24] S. Blundell, *Magnetism in Condensed Matter* (Oxford University Press, Oxford, 2003).
[25] N. Kim, H. Kim, J. W. Kim, S. J. Lee, and T. W. Kang, Phys. Rev. B **74**, 155327 (2006).
[26] B. Lee, T. Jungwirth, and A. H. MacDonald, Phys. Rev. B **61**, 15606 (2000).
[27] R. C. Myers, M. Poggio, N. P. Stern, A. C. Gossard, and D. D. Awschalom, Phys. Rev. Lett. **95**, 017204 (2005).
[28] J. C. Egues and J. W. Wilkins, Phys. Rev. B **58**, R16012 (1998).